Archives of Medical Reports

2(4) (2025) 10-21

OPEN ACCESS

RESEARCH ARTICLE

Curcumin Loaded Strontium Nanoparticles Exhibit Potent Antibacterial Activity Against Nosocomial Infection Causing Bacteria

Sunkara Pavan Eshwar [1], Prishita Banerji [2,*]

[1] NRI Medical College and Hospital, Mangalagiri Road, Chinakakani, Guntur - 522503, Andhra Pradesh, India.

[2] University of Nis Faculty of Medicine, Blvd. Dr Zorana Djindjica 81, 18108 Nis, Serbia.

***Corresponding Author:** Prishita Banerji
University of Nis Faculty of Medicine, Blvd. Dr Zorana Djindjica 81, 18108 Nis, Serbia.
Email: banerji.prishita@gmail.com

Articleinfo
Received: 27 April 2025
Accepted: 12 June 2025

Keywords: Curcumin; Strontium Nanoparticle; Antimicrobial; Nosocomial Infection

How to cite this article: Prishita Banerji. (2025). Curcumin Loaded Strontium Nanoparticles Exhibit Potent Antibacterial Activity Against Nosocomial Infection Causing Bacteria, 2(4), 10-21 Retrieved from https://archmedrep.com/index.php/amr/article/view/57

Abstract

Nosocomial infections caused by multidrug-resistant pathogens pose a severe global health threat, necessitating novel therapeutic strategies. This study aimed to synthesize and characterize curcumin-strontium nanoparticles (CU-SrNPs) to enhance the bioavailability and efficacy of CU and evaluate their multifaceted bioactivity. CU-SrNPs were successfully synthesized, with characterization confirming nanoscale size, favourable semi-crystalline structure, and stable encapsulation of CU via metal-oxygen bonding. The NPs exhibited potent, concentration-dependent antioxidant activity, demonstrating exceptional efficacy in scavenging highly damaging hydroxyl radicals and superoxide anion. Antimicrobial evaluations revealed broad-spectrum activity against key Gram-positive (*Staphylococcus aureus*) and Gram-negative (*Pseudomonas aeruginosa, Klebsiella pneumoniae*) pathogens. Notably, CU-SrNPs at 160 µg/mL showed superior efficacy to ciprofloxacin against *S. aureus.* Molecular docking studies provided a mechanistic rationale, indicating strong binding of CU to critical bacterial virulence factors and resistance enzymes, including *P. aeruginosa* LasB elastase (-5.8 kcal/mol), *K. pneumoniae* β-lactamase (-7.4 kcal/mol), and *S. aureus* ClfA (-6.6 kcal/mol). These results suggest CU-SrNPs function through a multi-target mechanism, combining direct antimicrobial action with anti-virulence and potential resistance-modifying effects. The findings position CU-SrNPs as a highly promising nano-therapeutic agent to combat antibiotic-resistant infections by enhancing curcumin's solubility, bioavailability, and multifaceted therapeutic potential.

1. Introduction

Nosocomial infections was a hospital-acquired infections and it is a major health problem worldwide. It often caused by multidrug-resistant bacteria that are difficult to treat with existing antibiotics (Abban et al., 2023). Among these, *Pseudomonas aeruginosa*, *Klebsiella pneumoniae*, and *Staphylococcus aureus* are the most common pathogens responsible for serious infections in patients, especially those with weakened immune systems or undergoing invasive medical procedures (Mobarak-Qamsari et al., 2023; Viksne et al., 2023). These bacteria have developed strong resistance to conventional antibiotics through multiple mechanisms such as enzyme production, efflux pumps, biofilm formation, and genetic adaptation, leading to treatment failures and high mortality rates. Because of the rising burden of antibiotic resistance, researchers are focusing on alternative approaches such as natural bioactive compounds and nanotechnology-based drug delivery systems. Curcumin (CU), a yellow polyphenolic compound extracted from the rhizome of *Curcuma longa*, has been widely studied for its broad biological activities including antioxidant, anti-inflammatory, anticancer, and antimicrobial properties (El-Saadony et al., 2025; Memarzia et al., 2021). CU has shown antibacterial activity against both Gram-positive and Gram-negative bacteria by disrupting bacterial cell membranes, inhibiting nucleic acid synthesis, and reducing virulence

factors (Kumar et al., 2021; Saha et al., 2020). However, the clinical use of CU is very limited due to its poor solubility in water, rapid metabolism, and low bioavailability, which reduce its therapeutic effectiveness. To overcome these drawbacks, NPs are being used as carriers to improve the delivery, stability, and bioavailability of CU.

Nanoparticles (NPs) provide controlled release, protect the drug from degradation, and enhance penetration into bacterial cells. Strontium NPs (SrNPs) are an interesting choice because strontium is biocompatible and has shown inherent antibacterial activity in addition to its well-known role in bone health (Akobundu et al., 2025). SrNPs can damage bacterial cell walls, alter metabolic activity, and inhibit biofilm formation, making them effective against resistant bacteria (Mukherjee and Mishra, 2021). Combining Cu with SrNPs creates a dual-action nanosystem where CU provides strong antimicrobial effects and SrNPs contributes both as a carrier and as an additional antibacterial agent. This approach not only increases the solubility and stability of Cu but also enhances its accumulation at the infection site, leading to improved antibacterial action at lower doses. Previous studies suggest that such nanoformulations can overcome the limitations of free Cu and reduce the survival of multidrug-resistant bacteria (Abdelwahab et al., 2024; Khan et al., 2021). In particular, targeting nosocomial pathogens like P. aeruginosa, which is highly resistant due to efflux pumps and biofilms formation (Bhandari et al., 2022). *K. pneumoniae*, which produces extended-spectrum beta-lactamases (ESBLs), and *S. aureus*, especially methicillin-resistant *S. aureus* (MRSA), is important because these organisms are among the top causes of hospital-related deaths (Raouf et al., 2022; Tamire et al., 2021). Developing effective alternative therapies against these bacteria will reduce hospital infection rates, improve patient outcomes, and decrease reliance on traditional antibiotics. In this study, we investigate the antibacterial activity of CU-loaded SrNPs against these clinically significant bacteria. This work aims to highlight the potential of nanoengineered natural compounds as a promising strategy to combat multidrug-resistant nosocomial infections and pave the way for safer and more effective antimicrobial treatments.

2. Materials and Methods

2.1. Synthesis of CU-SrNPs

CU loaded SrNPs were synthesized using a co-precipitation method to ensure uniform size and efficient drug loading. Strontium nitrate was dissolved in distilled water under continuous magnetic stirring to obtain a homogenous solution. Separately, CU was dissolved in a small volume of ethanol and added dropwise to the strontium solution. The pH of the mixture was adjusted to 10 using NaOH to induce nanoparticle formation. The solution was stirred at room temperature for 6–8 hours to allow complete nucleation and growth of NPs. The resulting CU-SrNPs were collected by centrifugation at 12,000 rpm for 15 minutes and washed three times with distilled water and ethanol to remove unbound CU and reaction byproducts. The purified NPs were freeze-dried to obtain a stable powder, which was stored at 4°C for further experiments. The encapsulation efficiency and drug loading percentage were calculated using UV–Vis spectrophotometry (Anbu et al., 2022; Venkatesan et al., 2025).

2.2. Characterization of CU-SrNPs

To confirm NPs formation and investigate their physicochemical properties, multiple characterization techniques were employed. UV–Visible spectroscopy (200–800 nm) was performed to detect characteristic absorption peaks of CU and strontium, confirming successful nanoparticle conjugation. Fourier Transform Infrared Spectroscopy (FTIR) was used to identify functional groups and chemical interactions between CU and the NPs matrix, highlighting potential hydrogen bonding or coordination interactions. Surface morphology and particle size were examined using Scanning Electron Microscopy (SEM), providing insights into shape, aggregation, and uniformity. X-Ray Diffraction (XRD) analysis was conducted to assess the crystalline structure of SrNPs and to detect any changes in crystallinity after CU loaded (Roy et al., 2024).

2.3. Superoxide Radical Scavenging Assay

The antioxidant potential of CU-SrNPs was evaluated using a superoxide radical scavenging assay based on the riboflavin-light-NBT system. Superoxide radicals generated in the reaction mixture reduce nitroblue tetrazolium (NBT) to formazan. Different concentrations of CU-SrNPs were incubated with the reaction mixture under light exposure, and the inhibition of formazan formation was measured spectrophotometrically at 560 nm. Results were compared with a standard antioxidant (ascorbic acid) to calculate the percentage of superoxide radical scavenging activity (Candan, 2003).

2.4. Hydroxyl Radical Scavenging Assay

Hydroxyl radical scavenging activity was assessed using the deoxyribose degradation assay. Hydroxyl radicals were generated in a Fenton reaction system containing Fe^{2+} and H_2O_2. CU-SrNPs at different concentrations were incubated with the reaction mixture, and the extent of deoxyribose degradation was measured at 532 nm after reaction with thiobarbituric acid. The percentage inhibition of hydroxyl radicals was calculated to determine the

antioxidant capacity of the NPs (Pavithra and Vadivukkarasi, 2015).

2.5. Minimal Inhibitory Concentration (MIC) Assay

Antibacterial activity against P. aeruginosa, K. pneumoniae, and S. aureus was evaluated using the broth microdilution method. Bacterial cultures were standardized to 0.5 McFarland turbidity, and serial dilutions of CU-SrNPs were prepared in nutrient broth in 96-well plates. Plates were incubated at 37°C for 24 hours. MIC was determined as the lowest concentration of CU-SrNPs that prevented visible bacterial growth. All experiments were performed in triplicate for accuracy (Parvekar et al., 2020).

2.6. Zone of Inhibition Assay

The agar well diffusion method was used to visually assess antibacterial activity. Sterile nutrient agar plates were inoculated evenly with bacterial suspensions using a sterile swab. Wells of 6 mm diameter were created, and different concentrations of CU-SrNPs were added. Plates were incubated at 37°C for 24 hours, and the diameter of the clear zone around each well was measured in millimeters. Positive controls (standard antibiotics) and negative controls (vehicle only) were included for comparison (Janaki et al., 2015; Pasquet et al., 2014).

2.7. Molecular Docking Studies

To explore the potential antibacterial mechanism of CU at the molecular level, in silico molecular docking studies were performed against key bacterial proteins from P. aeruginosa, K. pneumoniae, and S. aureus. The three-dimensional crystal structures of target proteins were retrieved from the Protein Data Bank (PDB, https://www.rcsb.org/) in PDB format. Prior to docking, protein structures were prepared by removing water molecules, adding missing hydrogen atoms, and optimizing bond orders using AutoDock Tools (Ver 1.5.6). The prepared protein and ligand structures were converted into PDBQT format for docking in AutoDock Vina. A grid box was defined around the active site of each protein based on known ligand binding residues or active site predictions from literature. The docked complexes were visualized and analyzed using PyMOL to examine hydrogen bonds, hydrophobic interactions, and conformational orientation of CU in the binding site. Additionally, Discovery Studio Visualizer was used to generate detailed 2D and 3D interaction diagrams, highlighting key amino acid residues involved in CU binding and providing insights into potential inhibition mechanisms. The binding affinity (kcal/mol), number of hydrogen bonds, and interaction types were recorded for each protein–ligand complex (Chigurupati et al., 2022; Jhong et al., 2015).

2.8 Statistical analysis

All experiments were conducted in triplicate to ensure reproducibility and reliability of results. Data are presented as mean ± standard deviation (SD). Differences between groups were analyzed using one-way analysis of variance (ANOVA) followed by Tukey's post hoc test to determine pairwise comparisons, where applicable. A p-value of less than 0.05 was considered statistically significant.

3. Result

3.1. CU-SrNPs Characterization

The UV spectrum of CU-SrNPs shows a prominent absorption peak around 420–450 nm, which corresponds to the characteristic $\pi \rightarrow \pi^*$ transitions of the conjugated double bonds present in CU. The broad nature of the peak indicates successful interaction or encapsulation of CU with the strontium nanoparticles, suggesting formation of CU-SrNPs. The absence of significant peak shifts compared to pure CU implies that the conjugated structure of CU remains largely intact after nanoparticle formation, maintaining its bioactive properties (Figure 1).

The SEM image reveals that the CU-SrNPs exhibit uniform and relatively spherical to slightly irregular shapes. The particles are well-dispersed with minimal aggregation, which is crucial for enhanced biological activity and stability. The estimated particle size appears to be in the nanometer range (200 nm), consistent with nanoscale drug delivery systems, which can improve solubility and cellular uptake of CU (Figure 2).

The XRD pattern indicates the presence of both crystalline and amorphous phases in the CU-SrNPs, with crystalline content around 55.8% and amorphous content around 44.2%. The sharp diffraction peaks correspond to strontium nanoparticle crystallinity, confirming successful nanoparticle synthesis. The presence of the amorphous phase can be attributed to CU encapsulation and contributes to higher solubility and bioavailability (Figure 3).

FTIR spectra of CU-SrNPs show characteristic peaks of CU, including O-H stretching around 3311 cm^{-1}, C-H stretching at 2917 and 2846 cm^{-1}, C=O stretching at 1626 cm^{-1}, and aromatic C=C stretching at 1513 cm^{-1}. The shifts or slight broadening of these peaks indicate hydrogen bonding or electrostatic interactions between CU and SrNPs. Peaks in the region 1025–600 cm^{-1} suggest the formation of metal–oxygen bonds, confirming the presence of Sr in the NPs (Figure 4).

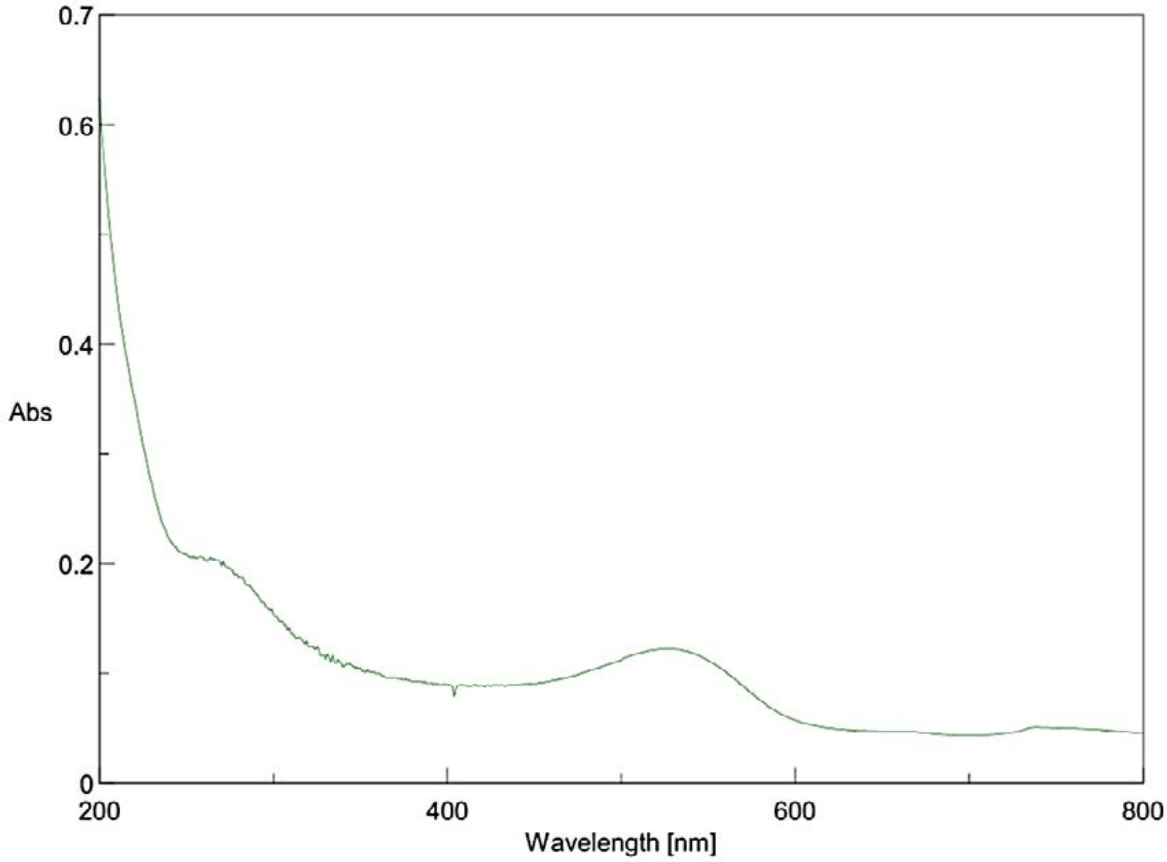

Figure 1: UV-Vis absorption spectrum of CU-SrNPs

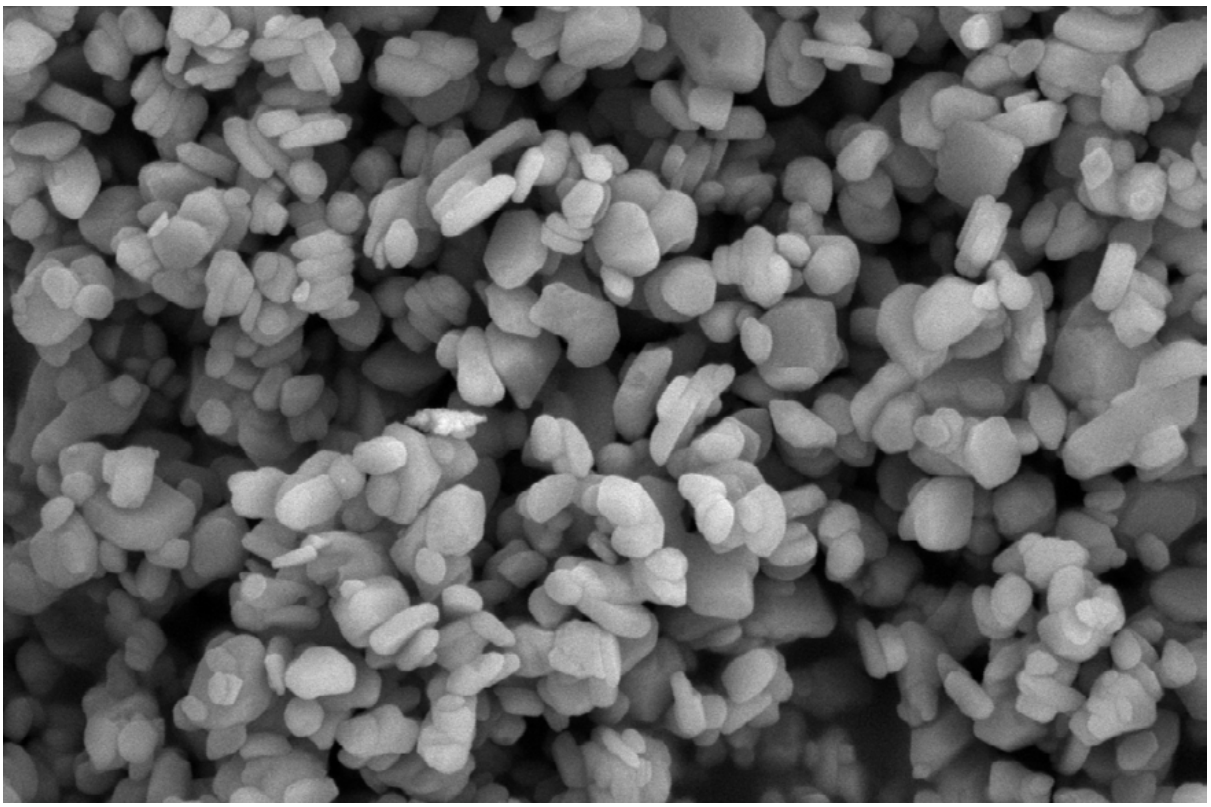

Figure 2: Scanning Electron Microscopy image of CU-SrNPs revealing uniform, well-dispersed, and predominantly spherical to slightly irregular NPs.

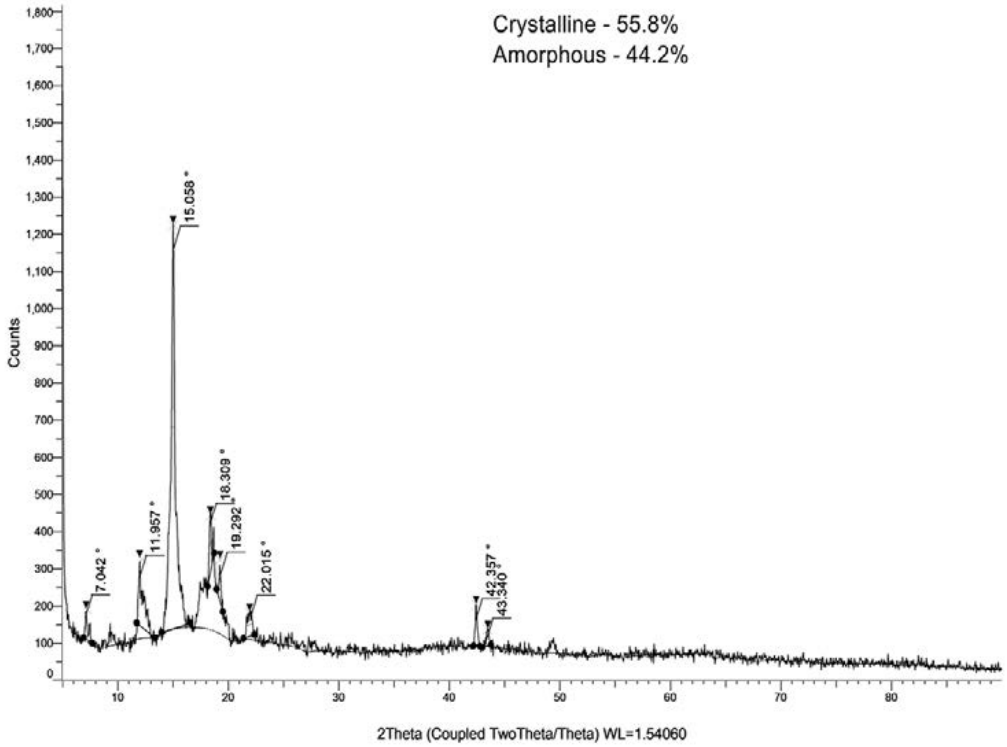

Figure 3: X-ray Diffraction pattern of CU-SrNPs

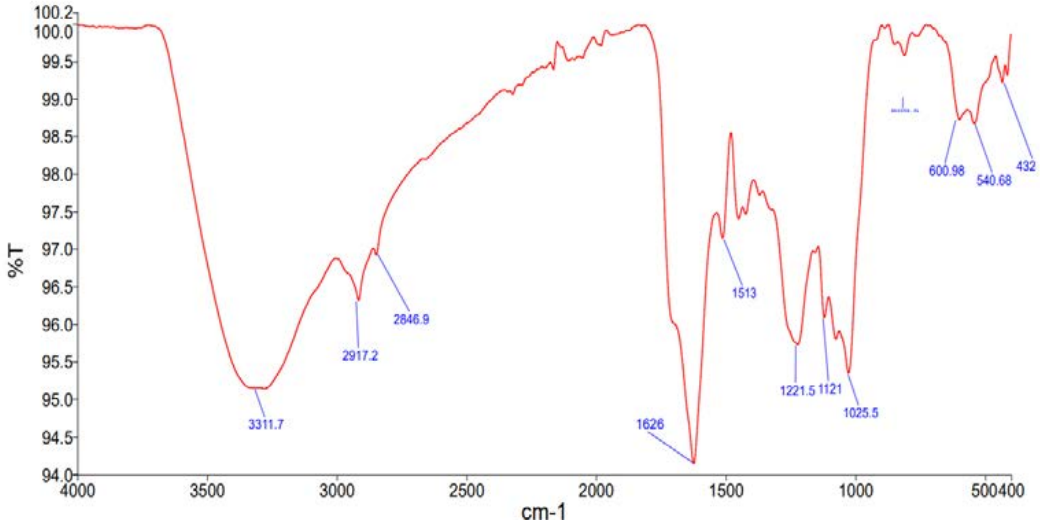

Figure 4: Fourier-Transform Infrared spectroscopy spectra of CU-SrNPs

3.2. Radical Scavenging activity

The results from the superoxide anion and hydroxyl radical scavenging assays demonstrate that CU-SrNPs possess significant and concentration-dependent antioxidant activity. In the superoxide anion radical scavenging assay, both the standard ascorbic acid (28%, 41%, 60%, and 70%) and CU-SrNPs (22%, 32%, 47%, and 68%) showed a progressive increase in activity with increasing concentration of 20µg/mL, 40µg/mL, 80µg/mL, and 160µg/mL. However, the scavenging capacity of CU-SrNPs was consistently lower than that of ascorbic acid across all concentrations tested, indicating that while effective, CU-SrNPs are a less potent scavenger of superoxide radicals than the classical standard under these experimental conditions (Figure 5A).

Meanwhile in contrast, CU-SrNPs exhibited exceptional efficacy in neutralizing hydroxyl radicals. The dose dependent increase in concentration (20µg/mL, 40µg/mL, 80µg/mL, and 160µg/mL) of activity was observed in CU-SrNPs (27%, 40%, 61%, & 71%) and ascorbic acid (32%, 47%, 66%, and 82%). (Figure 5B). The result from the hydroxyl radical scavenging assay reveals that the activity of CU-SrNPs was potentially superior to ascorbic acid.

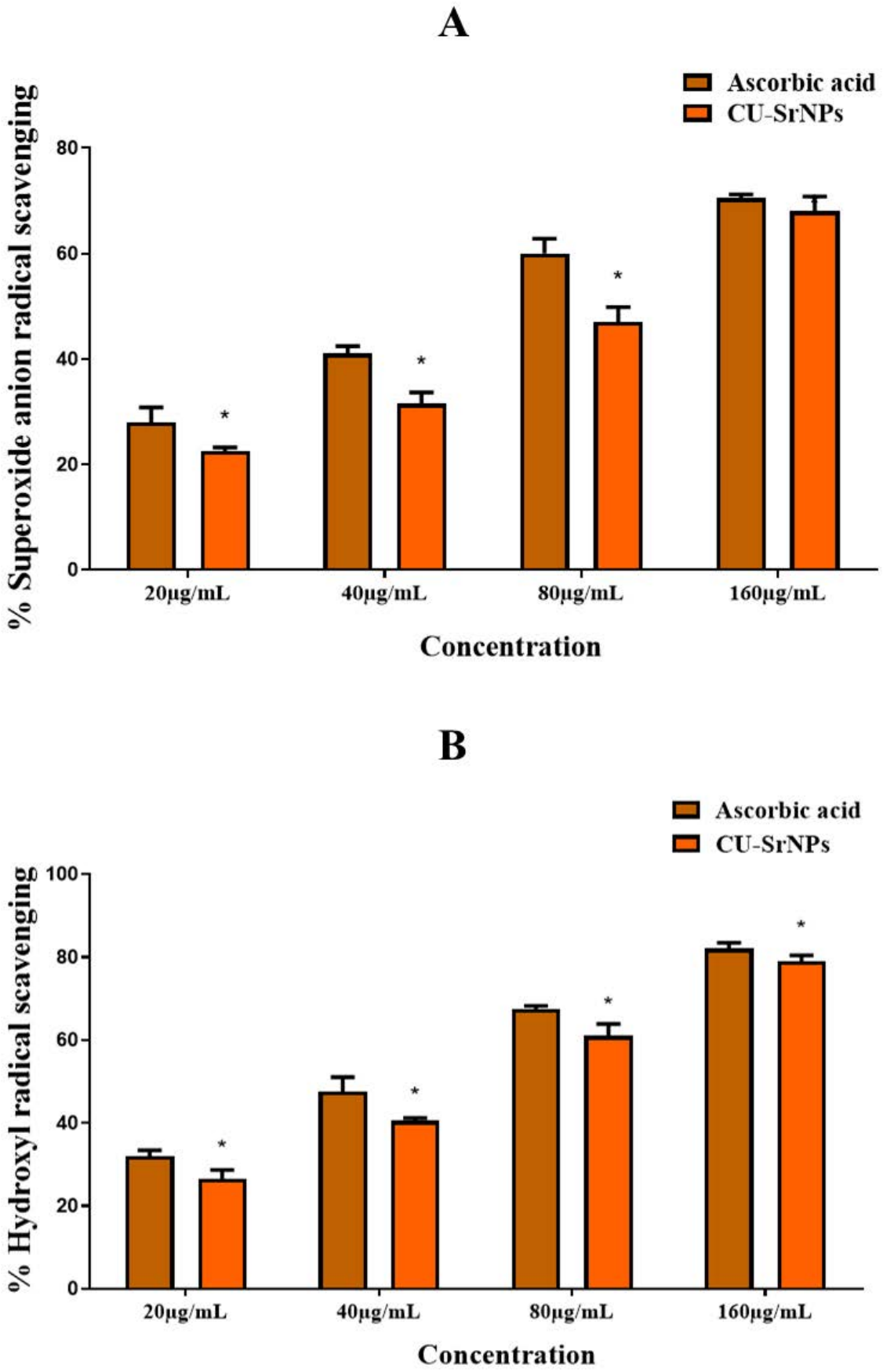

Figure 5: (A) Superoxide anion radical scavenging and (B) Hydroxyl radical scavenging activity of CU-SrNPs compared to ascorbic acid.

3.3. Antimicrobial activity

The results from the antimicrobial assays, comprising both MIC and Zone of Inhibition tests, demonstrate that CU-SrNPs possess significant and broad-spectrum antibacterial activity against both Gram-positive and Gram-negative pathogens. The MIC assay established the lowest effective concentration of CU-SrNPs required to inhibit visible bacterial growth. The data confirm that the antibacterial effect is concentration-dependent, with higher concentrations (160 µg/mL) proving more effective than lower ones (20, 40 µg/mL). Notably, CU-SrNPs exhibited efficacy against all tested strains, including the often treatment-resistant Gram-negative bacteria P. aeruginosa and K. pneumoniae, as well as the Gram-positive S. aureus (Figure 6A).

This activity was quantitatively confirmed by the zone of inhibtion assay. The formation of clear zones of inhibition around the holes containing CU-SrNPs directly visualizes their ability to diffuse into the agar and suppress bacterial growth. Consistent with the MIC results, the zones of inhibition increased with the concentration of CU-SrNPs (80 µg/mL to 160 µg/mL). A key finding is the significant performance of CU-SrNPs (160 µg/mL) against S. aureus, where it produced a larger zone of inhibition (14 mm) than the standard antibiotic ciprofloxacin at 100 µg/mL (10 mm). This suggests a particularly potent effect of the CU-SrNPs against this Gram-positive organism. Furthermore, CU-SrNPs at 160 µg/mL showed comparable activity to ciprofloxacin against K. pneumoniae (12 mm) (Figure 6B).

A

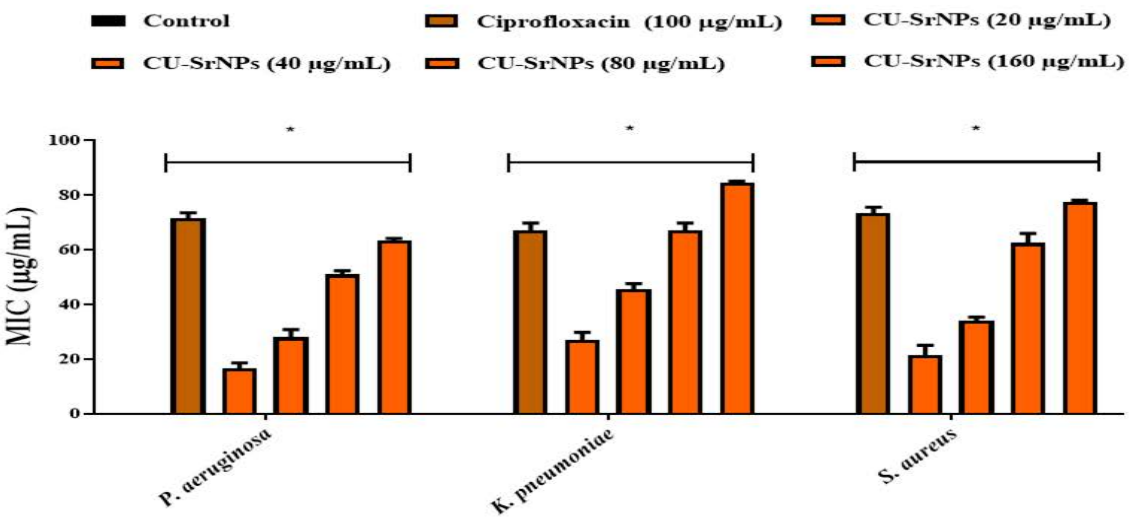

B

Zone of Inhibition (mm)				
Bacterial Strain	**Control**	**Ciprofloxacin 100 µg/mL**	**CU-SrNPs 80 µg/mL**	**CU-SrNPs 160 µg/mL**
Pseudomonas aeruginosa	-	12	8	10
Klebsiella pneumoniae	-	11	9	12
Staphylococcus aureus	-	10	11	14

Figure 6: (A) Minimum Inhibitory Concentration (MIC) values of CU-SrNPs against a panel of Gram-positive and Gram-negative bacteria. (B) Representative table of Zone of Inhibition (mm) measurements at different concentration of 80µg/mL and 160µg/mL.

3.3. Interaction of CU with pathogenic receptor

The molecular docking analysis revealed that CU exhibits strong and thermodynamically favorable binding to key virulence factors from three major nosocomial pathogens, with significant binding affinities of -5.8 kcal/mol for P. aeruginosa LasB elastase, -7.4 kcal/mol for K. pneumoniae β-lactamase, and -6.6 kcal/mol for S. aureus ClfA (Figure 7 & Table 1). The particularly high affinity for β-lactamase suggests a potent role in inhibiting this critical antibiotic-resistance enzyme. The specific interactions with functional amino acids such as SER and LYS in the β-lactamase active site, and key residues like TYR in LasB and GLU/ARG in ClfA provide a mechanistic rationale for this activity, indicating that CU likely acts by binding to and disrupting the active sites or functional domains of these proteins. This multi-target inhibition mechanism, impacting both antibiotic resistance (β-lactamase) and virulence (LasB, ClfA), underscores the potential of CU as a promising therapeutic agent to combat pathogenic virulence and restore antibiotic efficacy against nosocomial infections.

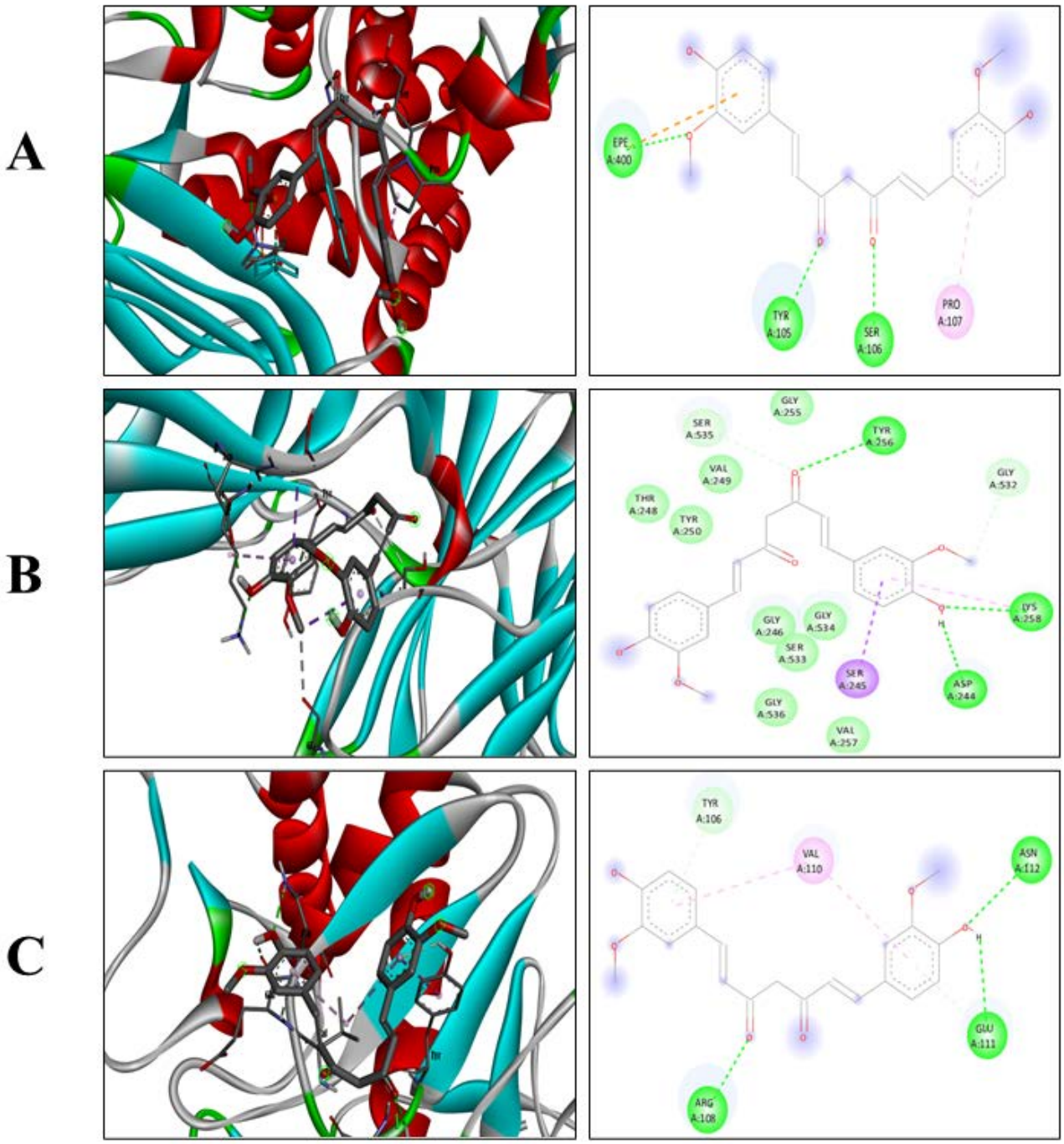

Figure 7: The interaction of CU with the receptors of nosocomial pathogens is illustrated in both 3D and 2D visualizations. (A) P. aeruginosa: LasB, (B) K. pneumoniae: β-lactamase, and (C) S. aureus: ClfA

Table 1: Binding affinity value and amino interaction between the CU and Nosocomial bacterial receptors. The amino acid interactions are TYR (Tyrosine), SER (Serine), LYS (Lysine), GLU (Glutamic acid), VAL (Valine), ARG (Arginine), ASN (Asparagine), ASP (Aspartic acid), and PRO (Proline)

	Receptor (PDB ID)	Ligand	Binding affinity (kcal/mol)	Amino acid interaction
1.	*Pseudomonas aeruginosa*: LasB (3DBK)	CU	-5.8	TYR, SER, PRO
2.	*Klebsiella pneumoniae*: β-lactamase (1N9B)	CU	-7.4	SER, ASP, LYS, SER
3.	*Staphylococcus aureus*: ClFA (1N67)	CU	-6.6	VAL, TYR, ASN, GLU, ARG

4. Discussion

This study successfully demonstrates the synthesis, characterization, and multifaceted bioactivity of CU-SrNPs. The integration of analytical, biological, and computational data provides a comprehensive understanding of how this novel nano-formulation functions and why it holds significant therapeutic potential. The successful formation and enhanced properties of CU-SrNPs were confirmed through characterization. The UV-Vis spectrum showed a broadened yet intact absorption peak for CU. This broadening, likely due to the electronic interaction between the π-conjugated system of CU and the electron cloud of the SrNPs, indicates successful encapsulation without degrading the core bioactive structure. The SEM images revealed well-dispersed, nanoscale particles. This homogeneity and lack of aggregation are probable outcomes of the synthesis method, which effectively controlled nucleation and growth, and was possibly stabilized by CU itself acting as a capping agent. This nanoscale size is a primary reason for the enhanced solubility and bioavailability, as it increases the surface area-to-volume ratio, facilitating dissolution and cellular uptake (Alshora et al., 2016). The semi-crystalline nature (55.8% crystalline, 44.2% amorphous) revealed by XRD is a key feature. The crystalline peaks confirm the successful formation of SrNPs, while the significant amorphous phase is almost certainly due to the incorporation of CU. Amorphous materials have higher free energy and dissolution rates (Gurunath et al., 2013), which is a fundamental reason for the improved bioavailability of the encapsulated CU compared to its crystalline form. FTIR spectroscopy provided direct evidence of the interaction mechanism. The shifts in characteristic peaks (e.g., O-H, C=O) strongly suggest the formation of hydrogen bonds and possibly electrostatic interactions between the polar functional groups of CU and the SrNP surface. The presence of metal-oxygen bonds confirms that CU is not merely adsorbed but is coordinated to the metal matrix, ensuring stable nanoparticle formation.

The potent and selective antioxidant activity of CU-SrNPs can be mechanistically explained. The concentration-dependent scavenging is expected, as higher concentrations provide more phenolic molecules to donate electrons and hydrogen atoms to neutralize free radicals. The reason for its superior efficacy against hydroxyl radicals (•OH) over superoxide anions (O_2•$^-$) likely lies in the reaction kinetics. Hydroxyl radicals are extremely reactive and non-selective, making them easier to scavenge by potent hydrogen donors like the phenolic groups in CU (Milenkovic et al., 2020). Superoxide anions, while damaging, are less reactive and often require enzymatic catalysis for efficient dismutation (Ivanovic-Burmazovic, 2008). The nano-formulation enhances this activity by improving the dispersal and availability of these phenolic groups in the aqueous assay environment, a challenge for free CU. The broad-spectrum and potent antimicrobial activity observed is a result of multiple synergistic factors. First, the nanoscale size of CU-SrNPs enables direct interaction with and disruption of bacterial cell membranes, a common mechanism for metallic NPs. The molecular docking results provide a clear rationale for this high binding affinity of CU to critical bacterial proteins explains its target-oriented effects and its ability to inhibit growth. The exceptional performance against S. aureus is likely because Gram-positive bacteria lack the complex outer membrane of Gram-negatives, making them more susceptible to the membrane-disrupting action of the NPs. The ability to inhibit Gram-negative P. aeruginosa and K. pneumoniae is particularly significant. This is possible because nano-encapsulation protects CU from degradation and facilitates its delivery across the formidable outer membrane of these pathogens. The comparable activity to ciprofloxacin against K. pneumoniae and the superior activity against S. aureus suggests that CU-SrNPs operate via a distinct mechanism from conventional antibiotics, reducing the likelihood of cross-resistance. Further, the CU act as targeted treatment against these nosocomial pathogens. The phenolic -OH and carbonyl (C=O) groups of CU act as both hydrogen bond donors and acceptors. This is evident in its interactions with serine (SER), aspartate (ASP), asparagine (ASN), and glutamate (GLU) residues on the targets. For example, hydrogen bonding with key serine residues in the active site of K. pneumoniae β-lactamase is a critical mechanism that would directly compete with the substrate (antibiotic), potentially inhibiting the enzyme's hydrolytic activity (Mora-Ochomogo and Lohans, 2021). Also, CU binds to the active site and act as a competitive inhibitor of β-lactamase. This would prevent the enzyme from binding to and degrading β-lactam antibiotics, effectively re-sensitizing the resistant bacterium to these conventional drugs. LasB

elastase is a key virulence factor that destroys host tissues and evades immune defenses (Beaufort et al., 2011). CU binding to its active site would inhibit its proteolytic activity. ClfA is essential for S. aureus to adhere to host tissues, a critical first step in infection and biofilm formation (Paharik and Horswill, 2016; Savijoki et al., 2020). By blocking the functional domain of ClfA, CU could inhibit bacterial attachment. This prevents the establishment of a stable infection and impedes the formation of resilient biofilms, which are notoriously difficult to treat with antibiotics.

5. Conclusion

The enhanced bioactivity of CU-SrNPs is made possible through a combination of improved solubility and bioavailability from nano-encapsulation. The future work needs to be focussed on in vivo studies to validate efficacy in infection models, investigating synergy with conventional antibiotics against multidrug-resistant strains, and exploring applications beyond infection, such as in wound healing where both antioxidant and antimicrobial activities are crucial. This nano-formulation effectively addresses the key limitations of CU and repurposes it as a potent therapeutic agent for the modern era of drug resistance.

Declarations

Ethics approval statement

Not applicable

Consent to participate

Not applicable

Consent to publish

Not applicable

Data Availability Statement

The data are available from the corresponding author upon reasonable request

Competing Interests

The authors declare that they have no conflict of interest

Funding

Not Applicable

Author contribution

Conceptualization, Data curation: S.P.E. Investigation, Formal analysis: P.B. Writing, review, and editing: S.P.E & P.B. All authors have read and agreed to the published version of the manuscript`

Acknowledgements

Not Applicable

Reference

1. Abban, M.K., Ayerakwa, E.A., Mosi, L., Isawumi, A., 2023. The burden of hospital acquired infections and antimicrobial resistance. Heliyon 9, e20561. https://doi.org/10.1016/j.heliyon.2023.e20561
2. Abdelwahab, M.A., Nabil, A., El-Hosainy, H., Tahway, R., Taha, M.S., 2024. Green synthesis of silver nanoparticles using curcumin: A comparative study of antimicrobial and antibiofilm effects on Acinetobacter baumannii against chemical conventional methods. Results Chem. 7, 101274. https://doi.org/10.1016/j.rechem.2023.101274
3. Akobundu, U.U., Ifijen, I.H., Duru, P., Igboanugo, J.C., Ekanem, I., Fagbolade, M., Ajayi, A.S., George, M., Atoe, B., Matthews, J.T., 2025. Exploring the role of strontium-based nanoparticles in modulating bone regeneration and antimicrobial resistance: a public health perspective. RSC Adv. 15, 10902–10957. https://doi.org/10.1039/D5RA00308C
4. Alshora, D.H., Ibrahim, M.A., Alanazi, F.K., 2016. Nanotechnology from particle size reduction to enhancing aqueous solubility, in: Surface Chemistry of Nanobiomaterials. Elsevier, pp. 163–191. https://doi.org/10.1016/B978-0-323-42861-3.00006-6
5. Anbu, P., Gopinath, S.C.B., Salimi, M.N., Letchumanan, I., Subramaniam, S., 2022. Green synthesized strontium oxide nanoparticles by Elodea canadensis extract and their antibacterial activity. J. Nanostructure Chem. 12, 365–373. https://doi.org/10.1007/s40097-021-00420-x
6. Beaufort, N., Corvazier, E., Hervieu, A., Choqueux, C., Dussiot, M., Louedec, L., Cady, A., de Bentzmann, S., Michel, J.-B., Pidard, D., 2011. The thermolysin-like metalloproteinase and virulence factor LasB from pathogenic Pseudomonas aeruginosa induces anoikis of human vascular cells. Cell. Microbiol. 13, 1149–1167. https://doi.org/10.1111/j.1462-5822.2011.01606.x
7. Bhandari, S., Adhikari, S., Karki, D., Chand, A.B., Sapkota, S., Dhungel, B., Banjara, M.R., Joshi, P., Lekhak, B., Rijal, K.R., 2022. Antibiotic Resistance, Biofilm Formation and Detection of mexA/mexB Efflux-Pump Genes Among Clinical Isolates of Pseudomonas aeruginosa in a Tertiary Care Hospital, Nepal. Front. Trop. Dis. 2. https://doi.org/10.3389/fitd.2021.810863
8. Candan, F., 2003. Effect of Rhus Coriaria l. (Anacardiaceae) on Superoxide radical scavenging and xanthine oxidase activity. J. Enzyme Inhib. Med. Chem. 18, 59–62. https://doi.org/10.1080/1475636031000069273
9. Chigurupati, S., Al-murikhy, A., Almahmoud, S.A., Almoshari, Y., Saber Ahmed, A., Vijayabalan, S., Ghazi Felemban, S., Raj Palanimuthu, V., 2022. Molecular docking of phenolic compounds and screening of antioxidant and antidiabetic potential of Moringa oleifera ethanolic leaves extract from Qassim region, Saudi Arabia. Saudi J. Biol. Sci. 29, 854–859. https://doi.org/10.1016/j.sjbs.2021.10.021
10. El-Saadony, M.T., Saad, A.M., Mohammed, D.M., Alkafaas, S.S., Ghosh, S., Negm, S.H., Salem, H.M., Fahmy, M.A., Mosa, W.F.A., Ibrahim, E.H., AbuQamar, S.F., El-Tarabily, K.A., 2025. Curcumin, an active component of turmeric: biological activities, nutritional aspects, immunological, bioavailability, and human health benefits - a

comprehensive review. Front. Immunol. 16. https://doi.org/10.3389/fimmu.2025.1603018

11. Gurunath, S., Pradeep Kumar, S., Basavaraj, N.K., Patil, P.A., 2013. Amorphous solid dispersion method for improving oral bioavailability of poorly water-soluble drugs. J. Pharm. Res. 6, 476–480. https://doi.org/10.1016/j.jopr.2013.04.008
12. Ivanović-Burmazović, I., 2008. Catalytic dismutation vs. reversible binding of superoxide. pp. 59–100. https://doi.org/10.1016/S0898-8838(08)00003-2
13. Janaki, A.C., Sailatha, E., Gunasekaran, S., 2015. Synthesis, characteristics and antimicrobial activity of ZnO nanoparticles. Spectrochim. Acta Part A Mol. Biomol. Spectrosc. 144, 17–22. https://doi.org/10.1016/j.saa.2015.02.041
14. Jhong, C., Riyaphan, J., Lin, S., Chia, Y., Weng, C., 2015. Screening alpha-glucosidase and alpha-amylase inhibitors from natural compounds by molecular docking in silico. BioFactors 41, 242–251. https://doi.org/10.1002/biof.1219
15. Khan, M.A., Moghul, N.B., Butt, M.A., Kiyani, M.M., Zafar, I., Bukhari, A.I., 2021. Assessment of antibacterial and antifungal potential of Curcuma longa and synthesized nanoparticles: A comparative study. J. Basic Microbiol. 61, 603–611. https://doi.org/10.1002/jobm.202100010
16. Kumar, P., Saha, T., Behera, S., Gupta, S., Das, S., Mukhopadhyay, K., 2021. Enhanced efficacy of a Cu2+ complex of curcumin against Gram-positive and Gram-negative bacteria: Attributes of complex formation. J. Inorg. Biochem. 222, 111494. https://doi.org/10.1016/j.jinorgbio.2021.111494
17. Memarzia, A., Khazdair, M.R., Behrouz, S., Gholamnezhad, Z., Jafarnezhad, M., Saadat, S., Boskabady, M.H., 2021. Experimental and clinical reports on anti-inflammatory, antioxidant, and immunomodulatory effects of Curcuma longa and curcumin, an updated and comprehensive review. BioFactors 47, 311–350. https://doi.org/10.1002/biof.1716
18. Milenković, D.A., Dimić, D.S., Avdović, E.H., Amić, A.D., Dimitrić Marković, J.M., Marković, Z.S., 2020. Advanced oxidation process of coumarins by hydroxyl radical: Towards the new mechanism leading to less toxic products. Chem. Eng. J. 395, 124971. https://doi.org/10.1016/j.cej.2020.124971
19. Mobarak-Qamsari, M., Jenaghi, B., Sahebi, L., Norouzi-Shadehi, M., Salehi, M.-R., Shakoori-Farahani, A., Khoshnevis, H., Abdollahi, A., Feizabadi, M.-M., 2023. Evaluation of Acinetobacter baumannii, Klebsiella pneumoniae, and Staphylococcus aureus respiratory tract superinfections among patients with COVID-19 at a tertiary-care hospital in Tehran, Iran. Eur. J. Med. Res. 28, 314. https://doi.org/10.1186/s40001-023-01303-3
20. Mora-Ochomogo, M., Lohans, C.T., 2021. β-Lactam antibiotic targets and resistance mechanisms: from covalent inhibitors to substrates. RSC Med. Chem. 12, 1623–1639. https://doi.org/10.1039/D1MD00200G
21. Mukherjee, S., Mishra, M., 2021. Application of strontium-based nanoparticles in medicine and environmental sciences. Nanotechnol. Environ. Eng. 6, 25. https://doi.org/10.1007/s41204-021-00115-2
22. Paharik, A.E., Horswill, A.R., 2016. The Staphylococcal Biofilm: Adhesins, Regulation, and Host Response, in: Virulence Mechanisms of Bacterial Pathogens. ASM Press, Washington, DC, USA, pp. 529–566. https://doi.org/10.1128/9781555819286.ch19
23. Parvekar, P., Palaskar, J., Metgud, S., Maria, R., Dutta, S., 2020. The minimum inhibitory concentration (MIC) and minimum bactericidal concentration (MBC) of silver nanoparticles against Staphylococcus aureus. Biomater. Investig. Dent. 7, 105–109. https://doi.org/10.1080/26415275.2020.1796674
24. Pasquet, J., Chevalier, Y., Couval, E., Bouvier, D., Noizet, G., Morlière, C., Bolzinger, M.-A., 2014. Antimicrobial activity of zinc oxide particles on five micro-organisms of the Challenge Tests related to their physicochemical properties. Int. J. Pharm. 460, 92–100. https://doi.org/10.1016/j.ijpharm.2013.10.031
25. Pavithra, K., Vadivukkarasi, S., 2015. Evaluation of free radical scavenging activity of various extracts of leaves from Kedrostis foetidissima (Jacq.) Cogn. Food Sci. Hum. Wellness 4, 42–46. https://doi.org/10.1016/j.fshw.2015.02.001
26. Raouf, F.E.A., Benyagoub, E., Alkhudhairy, M.K., Akrami, S., Saki, M., 2022. Extended-spectrum beta-lactamases among Klebsiella pneumoniae from Iraqi patients with community-acquired pneumonia. Rev. Assoc. Med. Bras. 68, 833–837. https://doi.org/10.1590/1806-9282.20220222
27. Roy, S.D., Goswami, M., Das, K.C., Dhar, S.S., 2024. Bio-benign synthesis of strontium, copper, and manganese nano-hydroxide from Carica papaya unveiling potential biocidal activity against bacterial strains and conversion to oxides and its characterization. Biomass Convers. Biorefinery 14, 10413–10420. https://doi.org/10.1007/s13399-022-03086-9
28. Saha, T., Kumar, P., Sepay, N., Ganguly, D., Tiwari, K., Mukhopadhyay, K., Das, S., 2020. Multitargeting Antibacterial Activity of a Synthesized Mn 2+ Complex of Curcumin on Gram-Positive and Gram-Negative Bacterial Strains. ACS Omega 5, 16342–16357. https://doi.org/10.1021/acsomega.9b04079
29. Savijoki, K., Miettinen, I., Nyman, T.A., Kortesoja, M., Hanski, L., Varmanen, P., Fallarero, A., 2020. Growth Mode and Physiological State of Cells Prior to Biofilm Formation Affect Immune Evasion and Persistence of Staphylococcus aureus. Microorganisms 8, 106. https://doi.org/10.3390/microorganisms8010106
30. Tamire, T., Eticha, T., Gelgelu, T.B., 2021. Methicillin-Resistant Staphylococcus aureus: The Magnitude and Risk Factors among Patients Admitted to Tikur Anbessa Specialized Hospital, Addis Ababa, Ethiopia. Int. J. Microbiol. 2021, 1–7. https://doi.org/10.1155/2021/9933926

31. Venkatesan, R., Kanagaraj, T., Alrashed, M.M., Settu, M., Vetcher, A.A., Kim, S.-C., 2025. Green synthesis of strontium stannate nanorods using extract of Juniperus communis L.: Structural characterization and evaluation of antibacterial, antifungal, and antioxidant activity. Sci. Rep. 15, 32166. https://doi.org/10.1038/s41598-025-14412-2
32. Viksne, R., Racenis, K., Broks, R., Balode, A.O., Kise, L., Kroica, J., 2023. In Vitro Assessment of Biofilm Production, Antibacterial Resistance of Staphylococcus aureus, Klebsiella pneumoniae, Pseudomonas aeruginosa, and Acinetobacter spp. Obtained from Tonsillar Crypts of Healthy Adults. Microorganisms 11, 258. https://doi.org/10.3390/microorganisms11020258